# Synthesis, Spectroscopic and Electrochemical Characterization of Different Isomer Types in Tetrazolatoindium(III) Porphyrins

**Roger Guilard,*[a] Nadine Jagerovic,[a] Alain Tabard,[a] Christine Naillon[b] and Karl M. Kadish*[b]**

[a] *Laboratoire de Synthèse et d'Electrosynthèse Organométalliques, associé au CNRS (U.R.A. 33), Université de Bourgogne, Faculté des Sciences Gabriel, 6, Boulevard Gabriel, 21100 Dijon, France*

[b] *Department of Chemistry, University of Houston, Houston, TX 77204-5641, USA*

The synthesis and characterization of nine indium(III) porphyrin complexes with three types of σ-bonded tetrazolato axial ligands are reported. The investigated compounds In(por)($N_4CR$) where R = $CMe_3$, $CH{=}CH_2$ or CH=CHCN and por = the dianion of 2,3,7,8,12,13,17,18-octaethylporphyrin (oep), 5,10,15,20-tetraphenylporphyrin (tpp) or 5,10,15,20-tetra-*p*-trifluoromethylphenylporphyrin (tfpp) were characterized by UV/VIS, IR and $^1H$ NMR spectroscopy as well as by electrochemistry. The $N_4CR$ ligand of a given M(por)($N_4CR$) complex can have the R group attached to either the 4 or 5 position of the tetrazolato ring and this is discussed in the present study with respect to the steric and electronic effects of the axial and equatorial ligands.

A cycloaddition reaction between metalloporphyrin azides and nitriles such as MeCN, EtCN, PhCN or *p*-$NO_2C_6H_4CN$ has been demonstrated to give tetrazolato complexes of the type M(por)($N_4CR$) and M(por)($N_4CR)_2$ where M = one of several different metals in the +3 or +4 oxidation state, R = Me, Et, Ph or $C_6H_4NO_2$-*p* and por = the dianion of 2,3,7,8,12,13,17,18-octaethylporphyrin (oep), 5,10,15,20-tetraphenylporphyrin (tpp) or 5,10,15,20-tetra-*p*-trifluoromethylphenylporphyrin (tfpp).[1-5] The final product may exist in one of two different isomeric forms and this was confirmed by a structural characterization of In(oep)($N_4CMe$) and In(oep)($N_4CPh$) which have the R group attached at the 4 or 5 position of the tetrazolato ring as shown in Scheme 1.[2,3]

The formation of a specific isomer type for a given M(por)($N_4CR$) or M(por)($N_4CR)_2$ complex should depend upon both the steric and electronic effects of the R group on the axial ligand. This is discussed in this paper which presents a spectroscopic and electrochemical characterization of complexes In(por)($N_4CR$) (por = oep, tpp or tfpp; R = $CMe_3$, $CH{=}CH_2$ or CH=CHCN). Each σ-bonded indium(III) porphyrin was characterized by UV/VIS, IR and $^1H$ NMR spectroscopy as well as by electrochemistry. These results are compared to those for previously characterized In(por)($N_4CR$) complexes and the data of all known indium(III) tetrazolato porphyrins are intercompared and discussed in terms of the specific porphyrin ring, the specific axial ligand, and the isomer type. The results are also discussed with respect to data for other main-group and transition-metal porphyrins of the type M(por)($N_4CR$) and M(por)($N_4CR)_2$ where M = Ge, Sn, Co or Fe.

## Experimental

*Chemicals.*—The synthesis and handling of each porphyrin was carried out under an argon atmosphere. Pivalonitrile ($NCCMe_3$) and acrylonitrile ($NCCH{=}CH_2$) were freshly distilled under an inert atmosphere. Commercial grade fumaronitrile (NCCH=CHCN) was used without further purification. Reagent grade methylene chloride ($CH_2Cl_2$, Fisher) was distilled over $P_2O_5$ for electrochemical studies. Tetrabutylammonium hexafluorophosphate and tetrabutylammonium perchlorate were purchased from Fluka and recrystallized from ethanol prior to use. The compounds In(oep)Cl,[6] In(tpp)Cl[7] and In(tfpp)Cl[6] were obtained by metallation of the corresponding free-base porphyrins, $H_2$por, using literature methods. They were then converted to the corresponding In(por)($N_3$) derivatives according to a general procedure.[2,3]

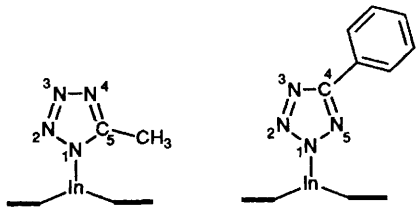


Scheme 1

*Preparation of the Tetrazolato Complexes.*—Complexes In(por)$N_3$ (300 mg) in toluene (50 $cm^3$) were mixed with nitrile (2 equivalents). The reaction mixture was refluxed and monitored by observing the disappearance of the azide band at 2070 $cm^{-1}$ by IR spectroscopy. The solution was then evaporated and the resulting crude solid recrystallized from toluene–heptane. In(oep)[$N_4C(CMe_3)$], yield = 78% (Found: C, 63.5; H, 6.8; N, 12.7. Calc. for $C_{41}H_{53}InN_8$: C, 63.7; H, 6.9; N, 14.5%). Chemical desorption ionization (DCI) MS: *m/z* 647 ([In(oep)]$^+$, 100), 772 ([In(oep){$N_4C(CMe_3)$}]$^{\cdot+}$, 1%). In(oep)[$N_4C(CH{=}CH_2)$], yield = 86% (Found: C, 62.7; H, 6.4; N, 15.1. Calc. for $C_{39}H_{47}InN_8$: C, 63.0; H, 6.4; N, 15.1%). DCI MS: *m/z* 647 ([In(oep)]$^+$, 100), 1389 ([In(oep){$N_4C(CH{=}CH_2)$} + In(oep)]$^+$, 1%). In(oep)[$N_4C$(CH=CHCN)], yield = 72% (Found: C, 61.8; H, 6.0; N, 10.9. Calc. for $C_{40}H_{46}InN_9$: C, 62.6; H, 6.0; N, 16.4%). DCI MS: *m/z* 647 ([In(oep)]$^+$, 100), 767 ([In(oep){$N_4C$(CH=CHCN)}]$^{\cdot+}$, 6%). In(tpp)[$N_4C(CMe_3)$], yield = 70% (Found: C, 69.0; H, 4.4; N, 11.2. Calc. for $C_{49}H_{37}InN_8$: C, 69.0; H, 4.4; N, 13.1%). DCI MS: 727 ([In(tpp)]$^+$, 100), 853 ([In(tpp){$N_4C(CMe_3)$} + H]$^+$, 1%). In(tpp)[$N_4C(CH{=}CH_2)$], yield = 50% (Found: C, 64.6; H, 4.1; N, 11.6. Calc. for $C_{47}H_{31}InN_8$: C, 68.6; H, 3.8; N, 13.6%). DCI MS: *m/z* 727 ([In(tpp)]$^+$, 100), 822 ([In(tpp){$N_4C(CH{=}CH_2)$} + H]$^+$, 1%). In(tpp)[$N_4C$(CH=CHCN)], yield = 66%

**Table 1** Infrared data ($\nu_{max}$/cm$^{-1}$) of the In(por)($N_4CR$) complexes (CsI pellet)

| Porphyrin | Axial ligand | $\nu_{max}$(R) | | | $\nu_{max}$(CN) | $\nu_{max}$(tetrazolato) | | | | | | | $\nu_{max}$(tetrazolato) + $\nu_{max}$(R) | | | |
|---|---|---|---|---|---|---|---|---|---|---|---|---|---|---|---|---|
| oep | $N_4C(CMe_3)$ | | | | | 1485 | | 1355 | | | 1190 | | | | | 490 |
| | $N_4C(CH{=}CH_2)$ | | 1639 | | | | 1410 | 1345 | | 1290 | | | 870 | 780 | 683 | 489 |
| | $N_4C(CH{=}CHCN)$ | 3050 | 1635 | | 2225 | 1495 | 1465 | 1385 | 1314 | 1295 | | 1035 | 800 | | | 465 |
| tpp | $N_4C(CMe_3)$ | 2960 | | | | 1485 | 1460 | | 1300 | | 1190 | | | | | 595 |
| | $N_4C(CH{=}CH_2)$ | | | | | 1490 | 1409 | | 1315 | 1260 | 1110 | | | | 732 | 466 |
| | $N_4C(CH{=}CHCN)$ | 3067 | 1635 | 960 | 2218 | 1495 | 1463 | 1385 | 1315 | 1294 | | | | | 730 | 416 |
| tfpp | $N_4C(CMe_3)$ | 2962 | | | | 1490 | 1405 | | | 1230 | | 984 | | | 728 | 462 |
| | $N_4C(CH{=}CH_2)$ | | | 940 | | 1480 | 1370 | | | 1240 | 1110 | | | | 725 | 690 |
| | $N_4C(CH{=}CHCN)$ | 3080 | 1645 | | 2226 | | | 1390 | 1270 | 1240 | | | | | | 530 |

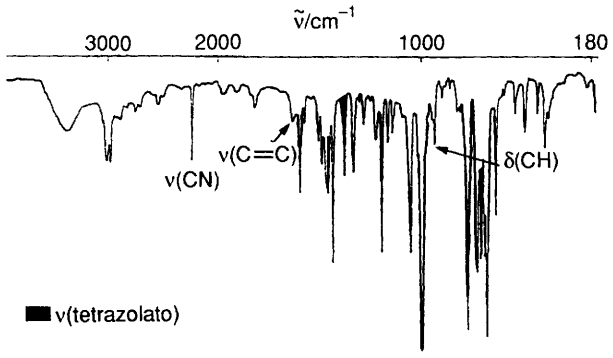


**Fig. 1** IR spectrum (CsI pellet) of In(tpp)[$N_4C(CH{=}CHCN)$]

(Found: C, 68.0; H, 3.7; N, 14.6. Calc. for $C_{48}H_{30}InN_9$: C, 68.0; H, 3.6; N, 14.9%). DCI MS: *m/z* 727 ([In(tpp)]$^+$, 100), 847 ([In(tpp){$N_4C(CH{=}CHCN)$}]$^{\cdot+}$, 7%). In(tfpp)[$N_4C(CMe_3)$], yield = 53% (Found: C, 56.6; H, 3.6; N, 7.9. Calc. for $C_{53}H_{33}F_{12}InN_8$: C, 56.6; H, 3.0; N, 9.9%). DCI MS: *m/z* 999 ([In(tfpp)]$^+$, 100%), 1124 ([In(tfpp){$N_4C(CMe_3)$}]$^{\cdot+}$, 1%). In(tfpp)[$N_4C(CH{=}CH_2)$], yield = 87% (Found: C, 55.5; H, 3.3; N, 10.3. Calc. for $C_{51}H_{27}F_{12}InN_8$: C, 55.9; H, 2.5; N, 10.2%). DCI MS: *m/z* 999 ([In(tfpp)]$^+$, 100%). In(tfpp)[$N_4C(CH{=}CHCN)$], yield = 31% (Found: C, 55.4; H, 2.4; N, 10.9. Calc. for $C_{52}H_{26}F_{12}InN_9$: C, 55.8; H, 2.3; N, 11.3%). DCI MS: *m/z* 999 ([In(tfpp)]$^+$, 100), 1119 ([In(tfpp){$N_4C(CH{=}CHCN)$}]$^{\cdot+}$, 6%).

*Physicochemical Measurements.*—Elemental analyses were performed by the Service de Microanalyse of the Centre National de la Recherche Scientifique. Mass spectra were recorded in the DCI mode using a VG TS 250 mass spectrometer. Proton NMR spectra were recorded at 400 MHz on a Bruker WM 400 spectrometer of the CSMUB (Centre de Spectrométrie Moléculaire de l'Université de Bourgogne). Spectra were measured from 5 mg solutions of the complex in deuteriated solvents with tetramethylsilane as internal reference. ESR spectra were recorded on an IBM model ER 100D spectrometer. The *g* values were measured with respect to diphenylpicrylhydrazyl ($g$ = 2.0036 ± 0.0003). Infrared spectra were obtained on a Perkin-Elmer 580 B apparatus. Solid samples were prepared as 1% dispersions in a CsI pellet. Electronic absorption spectra were recorded on a Perkin-Elmer 559 spectrophotometer, an IBM model 9430 spectrophotometer, or a Tracor Northern 1710 holographic optical spectrophotometer multichannel analyser.

Cyclic voltammograms were obtained with the use of a three-electrode system. The working electrode was a platinum button and a platinum wire was used as the counter electrode. A saturated calomel electrode (SCE) served as the reference electrode and was separated from the bulk of the solution by a fritted-glass bridge. All low-temperature electrochemical measurements were made with a non-isothermal cell in which the reference electrode was maintained at 20 ± 1 °C. A BAS 100 electrochemical analyser which was connected to a Houston Instrument HIPLOT DMP 40 plotter was used to measure the current–voltage curves.

Controlled potential electrolysis was performed with an EG&G model 173 potentiostat or a BAS 100 electrochemical analyser. Both the reference electrode and the platinum-wire counter electrode were separated from the bulk of the solution by means of a fritted-glass bridge. Thin-layer spectroelectrochemical measurements were performed with an IBM EC 225 voltammetric analyser coupled with a Tracor Northern 1710 spectrophotometer-multichannel analyser to give time-resolved spectral data. The utilized optically transparent platinum thin-layer electrode (OTTLE) is described in the literature.[8]

## Results

*Spectral Characterization of* In(por)($N_4CR$) *Complexes.*—The mass spectral data are consistent with the presence of a single axially bonded tetrazolato ligand (see Experimental section). A molecular-ion peak is seen for seven of the nine compounds, but not for In(oep)[$N_4C(CH{=}CH_2)$] or In(tfpp)-[$N_4C(CH{=}CH_2)$]. When observed, the molecular ion peak is of low intensity (1–7%). Similar results have been reported for five-co-ordinated carbon σ-bonded indium porphyrin derivatives[9] and this is consistent with a weak metal–axial ligand bond in these two types of complexes.

Infrared data of the In(por)($N_4CR$) complexes are summarized in Table 1 and an IR spectrum of In(tpp)[$N_4C(CH{=}CHCN)$] is shown in Fig. 1. This spectrum has a sharp band at 2218 cm$^{-1}$ which is attributable to a CN group.[10] Single sharp bands are also seen at 2225 or 2226 cm$^{-1}$ for the other two tetrazolato compounds formed after addition of NCCH=CHCN to In(por)($N_3$) and prove that only one of the two nitrile functionalities of fumaronitrile reacts with In(por)($N_3$). A similar result was reported earlier for cobalt tetrazolato porphyrins[5,11] and was explained by electronic effects of the tetrazolato ring on the second nitrile group.

Characteristic tetrazolato ring deformations[1–4,11–18] occur between 984 and 1495 cm$^{-1}$ and these bands are listed in Table 1. There are also typical tetrazolato ligand vibrations at lower wavenumbers as well as R-group vibrational frequencies in the same region (see Table 1). A $\delta_{CH}$ deformation vibration is located at 940 or 960 cm$^{-1}$ for two of the six complexes which contain vinyl groups while all three In(por)[$N_4C(CH{=}CHCN)$] species exhibit a CH stretching vibration of the CH=CHCN group at 3050–3080 cm$^{-1}$ (see Fig. 1 for the tpp complex). Bands at 1635–1645 cm$^{-1}$ are characteristic of C=C stretching vibrations while bands at 2960–2962 cm$^{-1}$ for In(tpp)[$N_4C(CMe_3)$] and In(tfpp)[$N_4C(CMe_3)$] can be assigned to the CH stretch of the methyl groups.[10]

The UV/VIS data for the complexes in tetrahydrofuran (thf) are summarized in Table 2. Each derivative has five major absorption bands. The spectra belong to the normal porphyrin class[19] and, in agreement with the known ionic character of the

**Table 2** UV/VIS data of the indium(III) porphyrin complexes in tetrahydrofuran

| | | $\lambda_{max}$/nm ($10^{-3}$ ε/dm$^3$ mol$^{-1}$ cm$^{-1}$) | | | | |
|---|---|---|---|---|---|---|
| Porphyrin | Axial ligand | B(1,0) | B(0,0) | Q(2,0) | Q(1,0) | Q(0,0) |
| oep | $N_4C(CMe_3)$ | 385(60.5) | 407(490.3) | 499(1.2) | 539(18.5) | 577(21.5) |
| | $N_4C(CH{=}CH_2)$ | 385(83.8) | 407(408.5) | 500(1.6) | 535(16.5) | 577(16.9) |
| | $N_4C(CH{=}CHCN)$ | 385(49.4) | 407(417.3) | 500(1.9) | 539(17.8) | 577(19.2) |
| tpp | $N_4C(CMe_3)$ | 403(36.5) | 425(490.8) | 520(2.5) | 560(18.4) | 600(8.9) |
| | $N_4C(CH{=}CH_2)$ | 403(33.9) | 425(578.5) | 520(2.9) | 560(18.8) | 600(10.0) |
| | $N_4C(CH{=}CHCN)$ | 405(91.7) | 426(700.3) | 521(3.1) | 559(24.5) | 600(12.9) |
| tfpp | $N_4C(CMe_3)$ | 402(40.5) | 423(590.0) | 520(2.2) | 559(20.5) | 598(7.5) |
| | $N_4C(CH{=}CH_2)$ | 402(38.3) | 425(598.5) | 520(2.9) | 559(20.6) | 599(7.8) |
| | $N_4C(CH{=}CHCN)$ | 403(41.5) | 424(580.0) | 520(2.9) | 560(20.9) | 599(7.6) |

**Table 3** Proton NMR data[a] of In(por)($N_4CR$) complexes (R = $CMe_3$, $CH{=}CH_2$ or CH=CHCN)

| | | | | Protons of $R^1$ | | Protons of $R^2$ | | Protons of R | |
|---|---|---|---|---|---|---|---|---|---|
| por | Axial ligand | $R^1$ | $R^2$ | | | | | | |
| oep | $N_4C(CMe_3)$ | H | Et | *meso*-H | s, 4, 10.39 | α-$CH_2$ | m, 8, 3.99 | $(CH_3)_3$ | s, 9, 0.11 |
| | | | | | | α′-$CH_2$ | m, 8, 3.86 | | |
| | | | | | | β-$CH_3$ | t, 12, 1.79 | | |
| | $N_4C(CH{=}CH_2)$ | H | Et | *meso*-H | s, 4, 10.41 | α-$CH_2$ | m, 8, 4.01 | CH | d, 1, 4.90 |
| | | | | | | α′-$CH_2$ | m, 8, 3.87 | CH | d, 1, 4.14 |
| | | | | | | β-$CH_3$ | t, 12, 1.79 | CH | *b* |
| | $N_4C(CH{=}CHCN)$[c] | H | Et | *meso*-H | s, 4, 10.39 (10.46) | α-$CH_2$ | m, 8, 4.01 (4.16) | CH | s, 1, 4.48 (d, 1, 4.84) |
| | | | | | | α′-$CH_2$ | m, 8, 3.89 (4.16) | CH | s, 1, 4.44 (d, 1, 2.91) |
| | | | | | | β-$CH_3$ | t, 12, 1.81 (1.97) | | |
| tpp | $N_4C(CMe_3)$ | Ph | H | *o*-H | m, 8, 8.05 | pyrrole H | s, 8, 9.04 | $(CH_3)_3$ | s, 9, 0.25 |
| | | | | *m,p*-H | m, 12, 7.45 | | | | |
| | $N_4C(CH{=}CH_2)$ | Ph | H | *o*-H | d, 4, 8.04 | pyrrole H | s, 8, 9.03 | CH | d, 1, 5.03 |
| | | | | *o*′-H | d, 4, 8.01 | | | $CH_2$ | m, 2, 4.31 |
| | | | | *m,p*-H | m, 12, 7.45 | | | | |
| | $N_4C(CH{=}CHCN)$[c] | Ph | H | *o*-H | m, 8, 8.11 (8.34) | pyrrole H | s, 8, 9.04 (9.15) | CH | s, 1, 4.77 (d, 1, 5.14) |
| | | | | *o*′-H | m, 8, 8.04 (8.15) | | | CH | s, 1, 4.77 (d, 1, 4.21) |
| | | | | *m,p*-H | m, 12, 7.47 (7.82) | | | | |
| tfpp | $N_4C(CMe_3)$ | *p*-$CF_3C_6H_4$ | H | *o*-H | d, 4, 7.89 | pyrrole H | s, 8, 8.86 | $(CH_3)_3$ | s, 9, 0.35 |
| | | | | *o*′-H | d, 4, 7.85 | | | | |
| | | | | *m*-H | d, 4, 7.70 | | | | |
| | | | | *m*′-H | d, 4, 7.67 | | | | |
| | $N_4C(CH{=}CH_2)$ | *p*-$CF_3C_6H_4$ | H | *o*-H | d, 4, 7.86 | pyrrole H | s, 8, 8.85 | CH | d, 1, 5.14 |
| | | | | *o*′-H | d, 4, 7.83 | | | CH | m, 1, 4.82 |
| | | | | *m*-H | d, 4, 7.69 | | | CH | d, 1, 4.36 |
| | | | | *m*′-H | d, 4, 7.67 | | | | |
| | $N_4C(CH{=}CHCN)$[c] | *p*-$CF_3C_6H_4$ | H | *o*-H | d, 4, 7.92 (8.48) | pyrrole H | s, 8, 8.87 (9.13) | CH | d, 1, 5.02 (d, 1, 5.19) |
| | | | | *o*′-H | d, 4, 7.88 (8.27) | | | CH | d, 1, 4.78 (br, 1, 4.72) |
| | | | | *m*-H | d, 4, 7.72 (8.13) | | | | |
| | | | | *m*′-H | d, 4, 7.68 (8.08) | | | | |

[a] Data given as multiplicity, intensity. Spectra were recorded in $C_6D_6$ at 21 °C with $SiMe_4$ as internal reference; chemical shifts downfield from $SiMe_4$ are defined as positive. Key: $R^1$ = porphyrin methinic group; $R^2$ = porphyrin pyrrole group; R = substituent of axial tetrazolato groups; s = singlet, d = doublet, t = triplet, m = multiplet, br = broad. [b] The signal cannot be observed due to the porphyrin $CH_2$ resonance. [c] Chemical shifts δ in $CDCl_3$ (at 21 °C) are given in parentheses.

co-ordinated tetrazolato ring,[1,2] closely resemble the spectra of In(por)($N_3$). The substituent R on the tetrazole has no major effect on the UV/VIS spectra but all bands of the tpp and tfpp complexes are red shifted when compared to the three oep species. This is due to the lower basicity of the tpp and tfpp macrocycles compared to that of oep.

Table 3 summarizes $^1$H NMR data of the In(por)($N_4CR$) complexes and a spectrum of In(tpp)[$N_4C$(CH=CHCN)] in $C_6D_6$ is reproduced in Fig. 2. The porphyrin chemical shifts of each complex are close to those of indium(III) porphyrins with anionic axial ligands such as $Cl^-$ or $ClO_4^-$.[20] A similarity between In(por)X (where X = an anionic ligand) and In(por)($N_4CR$) is also observed in the UV/VIS data[2,20] and this further supports an ionic-like metal–ligand bond in In(por)($N_4CR$).

Information about the co-ordination scheme of the indium metal is given by $^1$H NMR signal patterns of the porphyrin protons. An $ABX_3$ coupling is observed between the methylenic and methyl protons of the oep macrocycle. The aryl-group *ortho* protons of the two tetraarylporphyrin macrocycles appear as two doublet signals (Fig. 2) and this is explained by an inequivalence of the two porphyrin planes resulting from five-co-ordination by $In^{III}$ which lies above the mean porphyrin plane.[21] A comparison of frequency differences, $|\nu_A - \nu_B|$, for the three oep complexes indicates that the porphyrin plane inequivalence is independent of the specific tetrazolato axial ligand and suggests a similar metal–porphyrin plane distance in all three complexes.

The resonance of the $CMe_3$ group on In(por)[$N_4C(CMe_3)$] appears as a singlet between δ 0.11 and 0.35 (see Table 3) and varies only slightly with changes in electron donicity of the porphyrin macrocycle. As expected, the sequence of shifts follows the order: δ(tfpp) > δ(tpp) > δ(oep). The $^1$H NMR data indicate that the porphyrin ring current induces a shielding of the resonance frequencies but the $CMe_3$ shielding of In(por)[$N_4C(CMe_3)$] is lower than that for the Me or Et groups of In(por)($N_4CMe$) or In(por)($N_4CEt$).[2] The behaviour of In(por)[$N_4C(CH{=}CH_2)$] and In(por)[$N_4C$(CH=CHCN)] is also similar to that of In(por)[$N_4C(CMe_3)$].

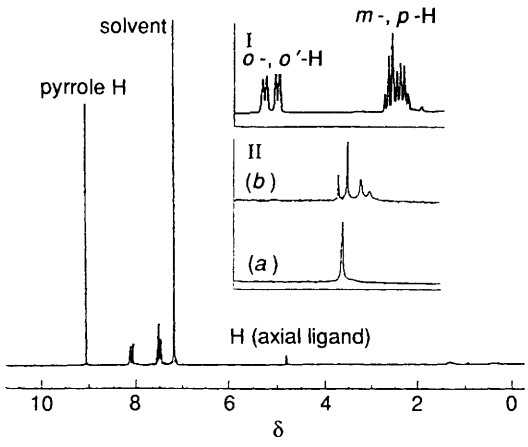


**Fig. 2** Proton NMR spectrum of In(tpp)[$N_4C$(CH=CHCN)] recorded at 21 °C in $C_6D_6$. Inset I is an expansion of the region δ 7.25–8.50 of this spectrum. Inset II shows the axial proton resonances (*a*) in $C_6D_6$ and (*b*) in $C_6D_6$–$CDCl_3$

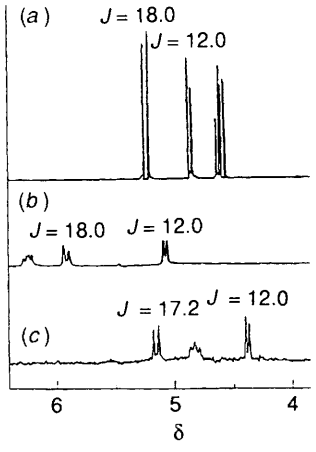


**Fig. 3** Proton NMR spectra recorded at 21 °C in $C_6D_6$ of (*a*) acrylonitrile; (*b*) the axial CH=$CH_2$ group of In(tfpp)[$N_4C$(CH=$CH_2$)] and (*c*) the vinyl protons of the $HN_4C$(CH=$CH_2$) substituted tetrazole, values of *J* in Hz

The NMR spectrum of acrylonitrile is shown in Fig. 3 which also illustrates the spectrum associated with the axial CH=$CH_2$ group of In(tfpp)[$N_4C$(CH=$CH_2$)] and the vinyl protons of unligated substituted tetrazole, $HN_4C$(CH=$CH_2$). This latter species was obtained by cleavage of the axial σ indium–nitrogen bond of In(por)[$N_4C$(CH=$CH_2$)] in the presence of hydrogen chloride. The typical $^3J_{trans}$ (≈18 Hz) and $^3J_{cis}$ (≈12 Hz) coupling constants are indicated in Fig. 3. A comparison of the different CH=$CH_2$ chemical shifts shows the small influence of the indium porphyrin ring current. The effect of the porphyrin macrocycle is also low since the CH=$CH_2$ and CH=CHCN protons give signals in the range of δ 4.14–5.14 and δ 4.44–5.02, respectively. In contrast, a strong solvent effect is observed. The signal for the axial ligand protons of In(tpp)[$N_4C$(CH=CHCN)] appears as a singlet in $C_6D_6$ but, as shown in Fig. 2, is split into a double doublet upon addition of $CDCl_3$. Smaller changes are observed for the other derivatives after addition of $CDCl_3$ to a solution of $C_6D_6$. A larger chemical shift difference between the two proton sites is systematically observed (see Table 3) and this could arise from the specific solvation of $CDCl_3$.

*Electrochemistry of* In(por)($N_4$CR).—Fig. 4 shows cyclic voltammograms of In(por)[$N_4C$($CMe_3$)] (por = tfpp, tpp or oep). All three compounds undergo two major reductions and a smaller third reduction is seen for the tpp and tfpp derivatives. The oep and tfpp complexes undergo only two oxidations but the tpp derivative shows three oxidations between 1.16 and 1.80

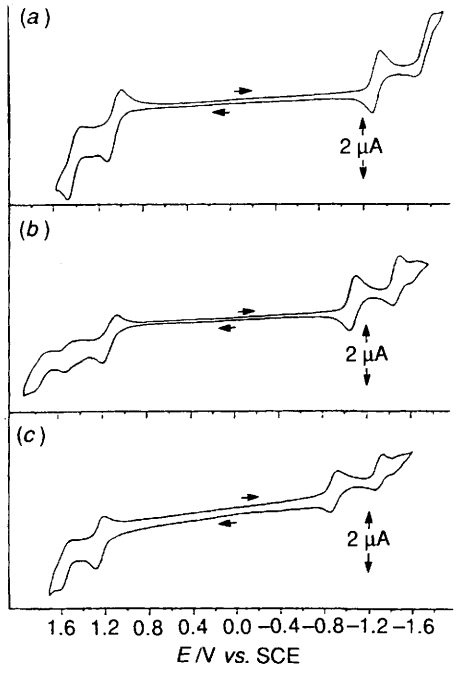


**Fig. 4** Cyclic voltammograms of In(por)[$N_4C$($CMe_3$)] for por = oep (*a*), tpp (*b*) or tfpp (*c*), in $CH_2Cl_2$, 0.1 mol $dm^{-3}$ $NBu_4ClO_4$. Scan rate = 100 mV $s^{-1}$

V. The newly synthesised In(por)($N_4$CR) derivatives exhibit electrochemical behaviour similar to what was earlier reported for In(por)($N_4$CR) complexes with other axial ligands[2] and the half-wave potentials for oxidation and reduction of all known tetrazolatoindium(III) porphyrins in $CH_2Cl_2$ are listed in Table 4.

Time-resolved UV/VIS spectra obtained during controlled-potential oxidation of In(oep)[$N_4C$($CMe_3$)], In(tfpp)[$N_4C$-(CH=$CH_2$)] and In(tpp)[$N_4C$($CMe_3$)] are shown in Fig. 5 and the resulting spectral data after controlled-potential oxidation of representative In(por)($N_4$CR) complexes are summarized in Table 5. The ESR spectra observed after the first oxidation of In(oep)[$N_4C$($CMe_3$)] and In(tpp)[$N_4C$(CH=CHCN)] are presented in Fig. 6. Both ESR spectra are consistent with a radical which is produced after the abstraction of two electrons at +1.25 V (oep) or at +1.30 V (tpp). The abstraction of one electron from the σ-bonded indium(III) complex should generate a porphyrin π-cation radical and the resulting data suggest that the electrooxidation and a cleavage of the tetrazolato axial ligand both occur on the bulk electrolysis time-scale. This is also suggested by the voltammetric data. For example, when a solution of In(oep)[$N_4C$($CMe_3$)] is bulk-oxidized at +1.25 V and then rereduced at 0.0 V, the cyclic voltammogram shows a reversible process at $E_{\frac{1}{2}}$ = 1.04 V. As seen in Table 4, this potential corresponds to $E_{\frac{1}{2}}$ for the first oxidation of In(oep)$ClO_4$.

Half-wave potentials for oxidation of representative complexes at −50 °C and 25 °C are summarized in Table 6. The first oxidation of all three complexes is cathodically shifted by 10–50 mV upon lowering the temperature, while the second oxidation is shifted by 60–100 mV in the same direction for the oep and tfpp derivatives and by a much larger 120–150 mV for In(tpp)($N_4$CR).

Each In(por)($N_4$CR) complex is characterized by two major reductions and a third process is also seen at room temperature for the tfpp and tpp derivatives where R = $CMe_3$ or CH=CHCN. The peaks for this latter reduction vanish at lower temperatures as illustrated in Fig. 7 for In(tpp)[$N_4C$(CH=CHCN)].

Fig. 8 presents time-resolved UV/VIS spectra obtained during the first reduction of In(oep)[$N_4C$($CMe_3$)] and the resulting spectral data after controlled-potential reduction of representative In(por)($N_4$CR) complexes are summarized in Table 5. Similar types of spectral changes are observed during

**Table 4** Half-wave potentials[a] (V *vs.* SCE) for the oxidation and reduction of In(por)($N_4CR$) and In(por)X in $CH_2Cl_2$ containing 0.1 mol $dm^{-3}$ $NBu_4ClO_4$

| | | Oxidation | | | | Reduction | | | | | |
|---|---|---|---|---|---|---|---|---|---|---|---|
| Porphyrin | Axial ligand | 1 | 2 | 3[c] | $\Delta E_{\frac{1}{2}}$ | 1 | 2 | 3 | $\Delta E_{\frac{1}{2}}$ | $\lvert E_{\frac{1}{2}}(ox) - E_{\frac{1}{2}}(red)\rvert$[b] | Ref. |
| oep | $N_4CMe$ | 1.01 | 1.46 | | 0.45 | −1.30 | −1.75 | | 0.45 | 2.31 | 2 |
| | $N_4CEt$ | 1.06 | 1.44 | | 0.38 | −1.25 | −1.72 | | 0.47 | 2.31 | 2 |
| | $N_4CPh$ | 1.03 | 1.49 | | 0.46 | −1.30 | −1.74 | | 0.44 | 2.33 | 2 |
| | $N_4C(C_6H_4NO_2\text{-}p)$ | 1.07 | | | | *d* | *d* | | | | 2 |
| | $N_4C(CMe_3)$ | 1.07 | 1.42 | | 0.35 | −1.31 | −1.75 | | 0.44 | 2.38 | This work |
| | $N_4C(CH{=}CH_2)$ | 1.10 | 1.45 | | 0.35 | −1.26 | −1.69 | | 0.43 | 2.36 | This work |
| | $N_4C(CH{=}CHCN)$ | 1.07 | 1.45 | | 0.38 | −1.29 | −1.72 | | 0.43 | 2.36 | This work |
| | $ClO_4^-$ | 1.04 | 1.44 | | 0.40 | *e* | *e* | | | | This work |
| tpp | $N_4CMe$ | 1.06 | 1.49 | 1.81 | 0.43 | −1.02[a] | −1.49 | | | | 2, This work |
| | $N_4CEt$ | 1.17 | 1.47 | 1.76 | 0.30 | −1.00 | −1.42 | | 0.42 | 2.17 | 2, This work |
| | $N_4CPh$ | 1.17 | 1.51 | | 0.34 | −1.08 | −1.47 | | 0.39 | 2.25 | 2 |
| | $N_4C(CMe)$ | 1.16 | 1.53 | 1.80 | 0.37 | −1.03 | −1.42 | | 0.39 | 2.19 | This work |
| | $N_4C(CH{=}CH_2)$ | 1.15 | 1.50[f] | 1.79 | 0.35 | −1.01 | −1.42 | | 0.41 | 2.16 | This work |
| | $N_4C(CH{=}CHCN)$ | 1.17 | 1.50[f] | 1.83 | 0.36 | −0.96 | −1.35 | −1.64 | 0.39 | 2.13 | This work |
| | $ClO_4^-$ | 1.18 | 1.52 | 1.74 | 0.34 | −1.05 | −1.42 | | 0.37 | 2.23 | This work |
| tfpp | $N_4CMe$ | 1.32 | 1.60 | | 0.28 | −0.89 | −1.26 | | 0.37 | 2.21 | 2 |
| | $N_4CPh$ | 1.32 | 1.62 | | 0.30 | −0.91 | −1.31 | | 0.40 | 2.23 | 2 |
| | $N_4C(C_6H_4NO_2\text{-}p)$ | 1.28 | 1.64 | | 0.36 | *g* | *g* | | | | 2 |
| | $N_4C(CMe_3)$ | 1.25 | 1.58 | | 0.33 | −0.89 | −1.28 | | 0.39 | 2.14 | This work |
| | $N_4C(CH{=}CH_2)$ | 1.28 | 1.63 | | 0.35 | −0.88[f] | −1.28 | | 0.40 | 2.16 | This work |
| | $N_4C(CH{=}CHCN)$ | 1.26 | 1.59 | | 0.33 | −0.81 | −1.22[f] | −1.48 | | 2.07 | This work |

[a] $E_p$ measured at a scan rate of 100 mV $s^{-1}$. [b] Absolute difference between $E_{\frac{1}{2}}$ for the first oxidations and the first reduction. [c] Third oxidation is due to reaction of isoporphyrin. [d] Two reductions of the *p*-$NO_2C_6H_4$ group occur in addition to the porphyrin ring centred reactions. The overall electrode reactions are located at $E_{pc} = -0.83$ V, $E_{\frac{1}{2}} = -1.11$ and $-1.31$ V for a scan rate of 100 mV $s^{-1}$. [e] Ill defined process. [f] Broad wave or combination of overlapping waves. [g] Four reactions are observed at $E_p = -0.80$ V and $E_{\frac{1}{2}} = -0.94$, $-1.11$ and $-1.31$ V.

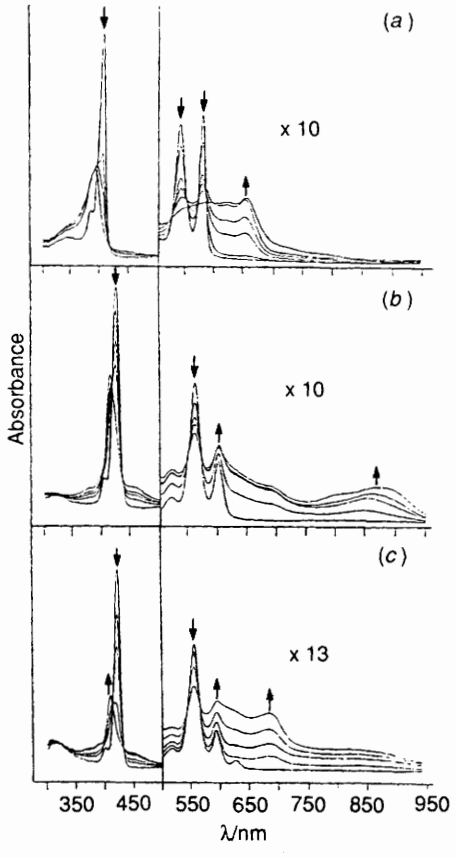


**Fig. 5** Time-resolved UV/VIS spectra taken during the first oxidation of (*a*) In(oep)[$N_4C(CMe_3)$], (*b*) In(tpp)[$N_4C(CMe_3)$] and (*c*) In(tfpp)[$N_4C(CH{=}CH_2)$] in $CH_2Cl_2$, 0.1 mol $dm^{-3}$ $NBu_4ClO_4$

the first reduction of each In(por)($N_4CR$) species. The Soret peak shifts from 406 to 420 nm upon a one-electron reduction of

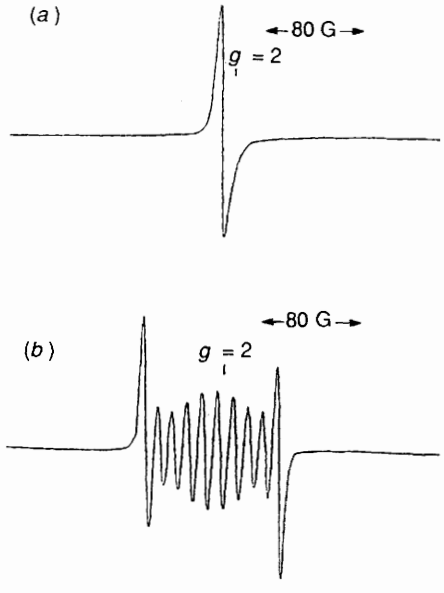


**Fig. 6** ESR spectrum recorded at 120 K after the first oxidation of In(oep)[$N_4C(CMe_3)$] and In(tpp)[$N_4C(CH{=}CHCN)$] in $CH_2Cl_2$, 0.1 mol $dm^{-3}$ $NBu_4ClO_4$

the oep complexes and a similar shift from 424 to 449 nm is observed after reduction of the tpp or tfpp derivatives. At the same time, the two Q bands in the visible region progressively disappear while two new peaks appear at 730 and 860 nm (tpp and tfpp complexes) or 635 and 815 nm for In(oep)[$N_4C(CMe_3)$].

The UV/VIS spectra obtained after the second reduction of In(tpp)($N_4CR$) or In(tfpp)($N_4CR$) are similar to those of the singly reduced complexes. The absorption bands remain at the same wavelength as for the singly reduced species but their intensities are generally decreased. The potentials for reduction of the oep complexes are close to the potential for solvent

**Table 5** Maximum absorbance wavelengths and corresponding molar absorption coefficients for neutral and reduced In(por)($N_4CR$) complexes in $CH_2Cl_2$ containing 0.1 mol $dm^{-3}$ $NBu_4ClO_4$

| Complex | Electrode reaction | $\lambda_{max}$/nm ($10^{-3}$ $\varepsilon$/$dm^3$ $mol^{-1}$ $cm^{-1}$) | | | | | | | |
|---|---|---|---|---|---|---|---|---|---|
| | | Soret region | | | | Q Bands | | | |
| In(oep)[$N_4C(CMe_3)$] | None | 385 (72) | 406 (523) | | | 537 (19) | 575 (20) | | |
| | Reduction 1 | | 408 (53) | 420 (59) | 447 (135) | | | 635 (14) | 815 (12) |
| | Oxidation 1 | 392 (204) | | | | | 595[a] (8) | | |
| In(oep)[$N_4C(CH{=}CH_2)$] | None | 385 (46) | 406 (509) | | | 536 (19) | 574 (20) | | |
| | Reduction 1 | | 409 (63) | 421 (56) | 448 (112) | | | 635 | *b* |
| | Oxidation 1 | 392 (168) | | | | | 595[a] | | |
| In(tpp)[$N_4C(CH{=}CHCN)$] | None | 402 (38) | 424 (531) | | | 557 (20) | 569 (9) | | |
| | Reduction 1 | | 427 (119) | 449 (154) | | | | 730 | *b* |
| | Reduction 2 | | 426 (60) | 451 (112) | | | | 730 | *b* |
| | Oxidation 1 | 414 (298) | 453 (48) | | | | 610[a] | | |
| In(tpp)[$N_4C(CMe_3)$] | None | 403 (46) | 424 (688) | | | 558 (22) | 597 (9) | | |
| | Reduction 1 | | 426 (185) | 449 (155) | | | | 730 (15) | 860 |
| | Reduction 2 | | 426 (72) | 452 (115) | | | | | 860 |
| | Oxidation 1 | 413 (320) | 455 (47) | | | 557 (14) | 598 (11) | | 860[a] |
| In(tfpp)[$N_4C(CH{=}CH_2)$] | None | 402 (44) | 423 (613) | | | 556 (22) | 595 (6) | | |
| | Reduction 1 | | 430 (125) | 449 (174) | | | | 720 | |
| | Reduction 2 | | | 451 (95) | | | | | |
| | Oxidation 1 | 412 (217) | | | | 556 (15) | 595 (12) | 681 (10) | |

[a] Broad band. [b] No data were obtained.

**Table 6** Temperature dependence on half-wave potentials for the oxidation of In(por)($N_4CR$) complexes in $CH_2Cl_2$ containing 0.1 mol $dm^{-3}$ $NBu_4ClO_4$

| Porphyrin | Axial ligand | $E_{\frac{1}{2}}$ at +20 °C | | | $E_{\frac{1}{2}}$ at −50 °C | | |
|---|---|---|---|---|---|---|---|
| | | 1 | 2[a] | 3[a] | 1 | 2 | 3 |
| oep | $N_4C(CMe_3)$ | 1.07 | 1.42 | | 1.07 | 1.35 | |
| | $N_4C(CH{=}CH_2)$ | 1.10 | 1.45 | | 1.08 | 1.35 | |
| | $N_4C(CH{=}CHCN)$ | 1.07 | 1.45 | | 1.06 | 1.37 | |
| tpp | $N_4C(CMe_3)$ | 1.16 | 1.53 | 1.80 | 1.14 | 1.39 | 1.68 |
| | $N_4C(CH{=}CH_2)$ | 1.15 | 1.50[b] | 1.79 | 1.12 | 1.38 | *c* |
| | $N_4C(CH{=}CHCN)$ | 1.17 | 1.53[b] | 1.83 | 1.12 | 1.38 | 1.69 |
| tfpp | $N_4C(CMe_3)$ | 1.25 | 1.58 | | 1.23 | 1.51 | |
| | $N_4C(CH{=}CH_2)$ | 1.28 | 1.63 | | 1.26 | 1.53 | |
| | $N_4C(CH{=}CHCN)$ | 1.26 | 1.59 | | 1.22 | 1.53 | |

[a] Quasireversible process. [b] Broad wave or combination of overlapping waves. [c] Ill defined process.

discharge and UV/VIS spectra were not obtained for any of the products formed after addition of a second electron to these species.

Exhaustive bulk controlled-potential reduction of In(tpp)[$N_4C(CH{=}CHCN)$] at −1.2 V gives the ESR spectrum shown in Fig. 9. The signal is centred at $g = 2.00$ and has a total width ($\Delta H$) of 160 G. Felton and Linschitz[22] have reported a broad signal for the π-anion radical of zinc(II) tetraphenylporphyrin but this species has a $\Delta H$ value of only 80–100 G and no splitting of the signal is observed. The ESR spectrum in Fig. 9 is almost identical to the one generated after controlled-potential reduction of In(tpp)$ClO_4$[20] and this suggests that the same singly reduced product is electrogenerated in solution. The half-wave potentials for reduction of In(tpp)[$N_4C(CH{=}CHCN)$] ($E_{\frac{1}{2}} = -0.96$ V) and In(tpp)$ClO_4$ ($E_{\frac{1}{2}} = -1.05$ V) differ by 90 mV and the thin-layer cyclic voltammogram shown in Fig. 10 is consistent with a cleavage of the tetrazolato axial ligand after electroreduction.

The In(tpp)($N_4CR$) electrochemistry differs from that of the oep and the tfpp derivatives in that three, rather than two, oxidations are observed in $CH_2Cl_2$ containing 0.1 mol $dm^{-3}$ $NBu_4ClO_4$ (see Table 4 and Fig. 4). The oxidation of In(por)($N_4CR$) is coupled to one or more chemical reactions and these occur after abstraction of the first and/or second electron. The final product is electroactive and a third reversible oxidation is seen between 1.74 and 1.83 V (see Table 4). There is also a new reduction which appears at $E_p = +0.48$ V for a scan rate of 100 mV $s^{-1}$. This latter peak is irreversible and only occurs after an initial oxidation of the complex, as illustrated in Fig. 11 for the case of In(tpp)[$N_4C(CMe_3)$].

## Discussion

It is now well known that many metal azides will undergo cycloaddition reactions with dipolarophiles.[5,23–27] As described in this paper and in the literature,[1–5] main-group and transition-metal azidoporphyrins of the type M(por)$N_3$ and M(por)$(N_3)_2$ can also react with nitriles and alkynes to give a tetrazolato or a triazolato metalloporphyrin complex. Sigma bonded tetrazolato porphyrins with seven different central metals have to date been synthesised and the unambiguously characterized species are listed in Table 7 as a function of isomer type.

Physicochemical properties[1–5] of the compounds in Table 7 suggest that the cycloaddition reaction depends upon both the nature of the dipolarophile and the type of azidometalloporphyrin starting compound. The data also show that the reaction time varies with the nature of the metal core. The reaction is faster with porphyrins containing a main-group central metal than with those which contain a transition metal. The change in polarizability of the co-ordinated azide must explain the different reactivity, *i.e.* the greater charge density of $In^{III}$, $Ge^{IV}$ or $Sn^{IV}$ compared to that of a transition metal such as $Co^{III}$[5] or $Fe^{III}$ will induce a more polarized metal-

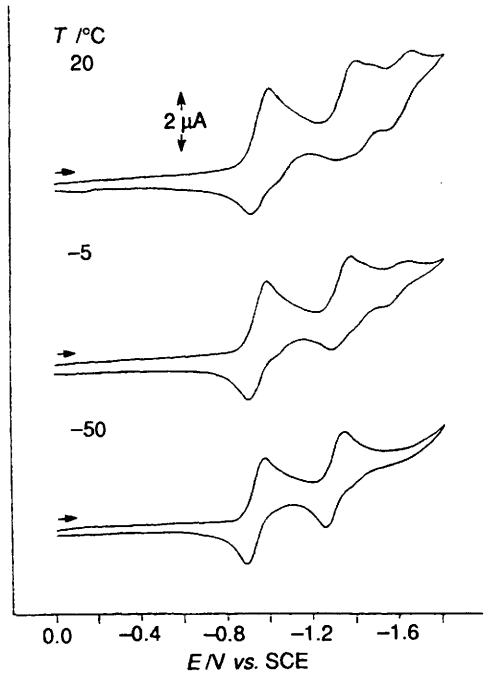


**Fig. 7** Cyclic voltammograms illustrating the reduction of In(tpp)[$N_4$-C(CH=CHCN)] in $CH_2Cl_2$, 0.1 mol $dm^{-3}$ $NBu_4ClO_4$, at different temperatures. Scan rate = 100 mV $s^{-1}$

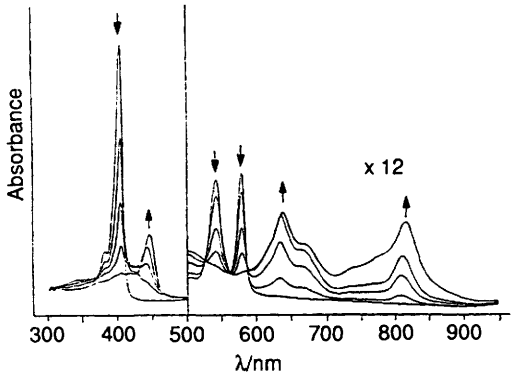


**Fig. 8** Time-resolved UV/VIS spectra taken during the first reduction of In(oep)[$N_4C(CMe_3)$] in $CH_2Cl_2$, 0.1 mol $dm^{-3}$ $NBu_4ClO_4$

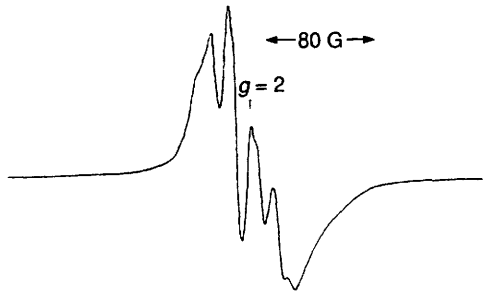


**Fig. 9** ESR spectrum recorded at 120 K after the first reduction of In(tpp)[$N_4C(CH=CHCN)$] in $CH_2Cl_2$, 0.1 mol $dm^{-3}$ $NBu_4ClO_4$

co-ordinated azide. Surprisingly, the basicity of the porphyrin macrocycle does not significantly affect the cycloaddition reaction to generate M(por)($N_4$CR) and this is most clearly demonstrated in the indium series.

The effect of the porphyrin macrocycle on the cycloaddition is not totally clearcut for the transition-metal porphyrins. Several side reactions can occur, with one example being the formation of a μ-nitrido iron(III) porphyrin dimer.[28,29] Another parameter which will affect the reaction rate is the polarizing character of the dipolarophile. This property is usually observed in the

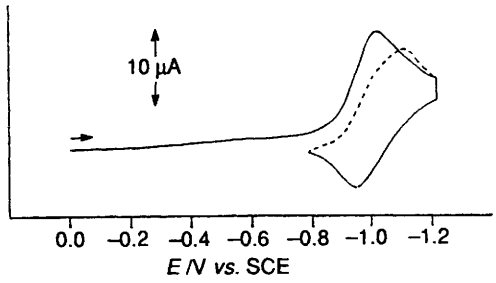


**Fig. 10** Thin-layer cyclic voltammogram on first scan (——) and second scan (– – –) for the reduction of In(tpp)[$N_4C(CH=CHCN)$] in $CH_2Cl_2$, 0.1 mol $dm^{-3}$ $NBu_4ClO_4$

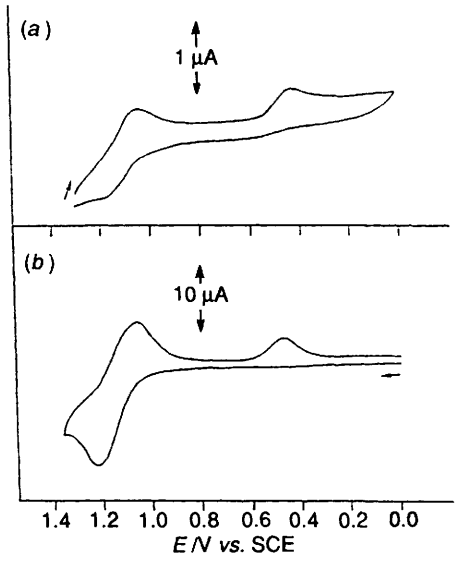


**Fig. 11** Cyclic voltammogram of In(tpp)[$N_4C(CMe_3)$] in $CH_2Cl_2$, 0.1 mol $dm^{-3}$ $NBu_4ClO_4$ (*a*) after bulk controlled-potential oxidation at +1.3 V (scan rate = 100 mV $s^{-1}$) and (*b*) before oxidation in a thin-layer cell (scan rate = 10 mV $s^{-1}$)

**Table 7** Tetrazolato complexes in the M(por)($N_4$CR)$_n$ ($n$ = 1 or 2) series

| M | por | R | Isomer type | Ref. |
|---|---|---|---|---|
| $Ge^{IV}$ | oep, tmtp, tptp | Ph | 2 | 4 |
| $Sn^{IV}$ | oep, tmtp, tptp | Ph | 2 | 4 |
| $In^{III}$ | oep, tpp, tfpp | Me | 1 | 2 |
| | oep, tpp, tfpp | Et | 1 | 2 |
| | oep, tpp, tfpp | $CMe_3$ | 2 | This work |
| | oep, tpp, tfpp | $CH{=}CH_2$ | 2 | This work |
| | oep, tpp, tfpp | CH=CHCN | 2 | This work |
| | oep, tpp, tfpp | Ph | 2 | 2 |
| | oep, tpp, tfpp | $C_6H_4NO_2$-*p* | 2 | 2 |
| $Fe^{III}$ | oep, tmp | Me | 1 | 1 |
| | oep | Et | 1 | 1 |
| | oep, tmp | Ph | 2 | 1 |
| | oep | $C_6H_4Me$-*p* | 2 | 1 |
| | oep | $C_6H_4Me$-*p* | 2 | 1 |

Abbreviations: tmtp = tetra-*m*-tolylporphyrinate; tptp = tetra-*p*-tolylporphyrinate; tmp = tetramesitylporphyrinate.

chemistry of metal co-ordinated azides,[27] where the least electron-rich nitriles are the most reactive.

Two different substitution isomers are possible for a given M(por)($N_4$CR) or M(por)($N_4CR)_2$ complex. These are labelled as isomer 1 and 2 in Scheme 2 for the mono-ligated species and involve attachment of the R group at the 4 or 5 position of the tetrazolato ligand.

The physicochemical data indicate that only a single com-

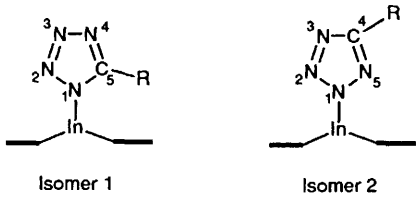


Scheme 2

pound is formed for a given tetrazolato complex independent of the dipolarophile or the porphyrin.[1-5] However, the structure of the isolated complex will depend upon the nature of the dipolarophile as illustrated in the indium porphyrin series for In(oep)($N_4$CMe) and In(oep)($N_4$CPh), both of which have been structurally characterized.[2,3] As indicated in Table 7, the methyl groups of Fe(por)($N_4$CMe) or In(por)($N_4$CMe) are in the 5 position but the phenyl groups of M(por)($N_4$CPh) or M(por)($N_4$CPh)$_2$ are in the 4 position of the tetrazolato ligand. This is also true for all of the porphyrin complexes containing In, Fe, Ge or Sn as central metals.

The isomer types for the indium porphyrins listed in Table 7 were assigned on the basis of $^1$H NMR data as well as by comparison with data for compounds which had been characterized on the basis of X-ray studies. The axial methyl group of In(oep)($N_4$CMe) is shielding by 1.38 ppm compared to the signal for MeCN [$\delta(CH_3)$ 1 in $C_6D_6$]. This is in contrast to the low shielding observed for the $CH_2$=CH group of In(oep)-[$N_4$C(CH=$CH_2$)] ($\Delta\delta \leqslant 0.7$) when compared to the signals of acrylonitrile ($\delta$ = 4.5, 4.8 and 5.2 in $C_6D_6$). A similar low shielding is observed between the *tert*-butyl substituent of In(oep)[$N_4$C($CMe_3$)] and $Me_3$CCN ($\Delta\delta$ = 0.9) as well as between the NCCH=CH group of In(oep)[$N_4$C(CH=CHCN)] and NCCH=CHCN ($\delta$ 4.2 in $C_6D_6$). This suggests that all three groups are at the 4 position of the co-ordinated tetrazolato ligand. Assignments for other aryl substituted derivatives such as *p*-$NO_2C_6H_4$, *p*-$MeC_6H_4$ or *m*-$MeC_6H_4$ were made by comparison with the NMR data of the phenyl signals of M(oep)($N_4$CPh) which has been studied by X-ray diffraction.[2,3]

The specific tetrazolato isomer which results from reaction of a given nitrile with the co-ordinated azide of M(por)$N_3$ or M(por)($N_3$)$_2$ is independent of both the porphyrin macrocycle and the specific central metal. The main parameter appears to be the nature of the nitrile reactant. Reactions with aryl or vinyl nitriles lead to the formation of isomer 2, while isomer 1 is formed in reactions involving an alkyl nitrile. Surprisingly, isomer 2 is also generated from In(por)$N_3$ and NCC$Me_3$ (see Table 7). This suggests that two effects must be taken into account. The first is the electron withdrawing character of the nitrile while the second is the steric effect of the R group. The results are as expected if one considers the formation of an intermediate three-centred activated complex[15,17] as represented in Scheme 3.

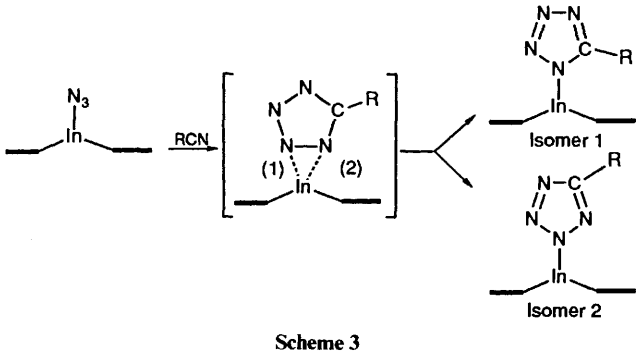


Scheme 3

The first step in Scheme 3 depends mainly on the electronic properties of the nitrile. This is best demonstrated by the Group 14 metalloporphyrins where neither Ge(por)($N_3$)$_2$ nor Sn(por)($N_3$)$_2$ reacts with acetonitrile but the expected tetrazolato product is formed in a reaction involving benzonitrile.[4]

The second step in the formation of a specific isomer type will depend on the relative stability of the (1) or (2) indium–nitrogen(tetrazolato) bond. The nucleophilicities of each nitrogen atom must be close to each other.[30] In addition, they must also be only slightly affected by the electron withdrawing properties of the tetrazolato substituent. The electron-withdrawing *p*-$NO_2C_6H_4$ substituent leads to formation of isomer 2 (see Table 7) and this is also the case for complexes with the strongly electron-donating $CMe_3$ group. Surprisingly, only a single isomer is obtained for a given In(por)($N_4$CR) complex. The expected isomer 1 cycloaddition product is isolated for the methyl and ethyl substituted tetrazolato complexes, but derivatives with R = $CMe_3$, CH=$CH_2$, CH=CHCN as well as those with an aryl group are sterically hindered and only isomer 2 is formed (see Table 7).

In summary, the occurrence of a cycloaddition reaction to give tetrazolato complexes shows that it is possible to involve metalloporphyrin axial ligands in a classical organic synthesis. In addition, the fact that numerous tetrazolato derivatives can be synthesised demonstrates that the specific metalloporphyrin does not significantly affect the nature of the final product. On the other hand, the reactivity of the co-ordinated azide ligand will depend upon the electronic properties of the porphyrin central metal and this is slightly modulated by the porphyrin macrocycle basicity. However, of most importance is the relative steric hindrance of the porphyrin ring with the $N_4$CR axial ligand and this seems to direct the formation of a specific final tetrazolato isomer.

*Electrochemistry*.—The electrochemistry of In(por)($N_4$CR) complexes is characterized by an initial formation of $\pi$-anion and $\pi$-cation radicals. The absolute potential difference between the first reduction and the first oxidation of each complex varies between 2.07 and 2.38 V in $CH_2Cl_2$ and this separation is consistent with data for other metalloporphyrins where only porphyrin ring centred reactions are observed.[31] The difference between the first and second reduction of a given In(por)($N_4$CR) species ranges between 0.32 and 0.43 V while the measured $\Delta E_{\frac{1}{2}}$ between the first and the second oxidations varies between 0.28 and 0.47 V. These data indicate that all four electrode reactions involve $\pi$ orbitals of the metalloporphyrin ring.[31]

There is no significant ligand dependence on $E_{\frac{1}{2}}$ for reduction or oxidation of complexes with different tetrazolato axial ligands and the same porphyrin ring. There is also no obvious trend between the donor–acceptor properties of the R substituent on In(por)($N_4$CR) and the structural characteristics of the porphyrin, *i.e.* the presence of isomer 1 or isomer 2. This suggests that the R group is too far away from the site of electron transfer (*i.e.* the porphyrin $\pi$ ring system) significantly to affect these processes. On the other hand, the half-wave potentials for each electrode reaction shift in a cathodic direction upon going from In(tfpp)($N_4$CR) to In(tpp)($N_4$CR) to In(oep)($N_4$CR) and this can be accounted for by the porphyrin ring basicity which increases in the order tfpp < tpp < oep.

The electrochemistry and spectroscopic properties of oxidized and reduced indium(III) porphyrins of the form In(por)X where por = tpp or oep and X = $Cl^-$ of $ClO_4^-$ have previously been reported.[20] The final product of reduction of In(tpp)Cl on the thin-layer spectroelectrochemical time scale (about 1 min) is a neutral In(tpp) radical and a similar product is suggested by the spectra of singly reduced In(por)($N_4$CR) in $CH_2Cl_2$. The thin-layer electrochemical data are also consistent with a cleavage of the metal–axial ligand bond after the first reduction. This is shown by the thin-layer cyclic voltammogram of In(tpp)[$N_4$C-(CH=CHCN)] in Fig. 10. As seen in this figure, a second reductive scan taken after holding the potential for 2.5 min at −1.2 V (a value just negative of $E_{\frac{1}{2}}$ for the first reduction) results in a new reduction process located at $E_{\frac{1}{2}}$ = −1.05 V. This value

is identical to $E_{\frac{1}{2}}$ for the first reduction of In(tpp)$ClO_4$ in $CH_2Cl_2$ (see Table 4). Based on these results, it can be concluded that the indium–tetrazolato ligand bond breaks after the first reduction of In(tpp)($N_4CR$). The final reduction product is In(tpp) and a reoxidation of this π-anion radical leads to In(tpp)$ClO_4$ rather than the original σ-bonded complex.

The electrochemically initiated conversion of In(por)($N_4CR$) to In(por)$ClO_4$ is not limited to tpp complexes and a similar sequence of steps is also observed for the three tfpp derivatives. The first reduction of In(tfpp)[$N_4C(CH{=}CH_2)$] occurs at $E_{\frac{1}{2}} \approx -0.89$ V but a new set of peaks is obtained at $E_{\frac{1}{2}} = -0.93$ V after an initial potential sweep past the first reduction. This new redox process is assigned as the reduction and oxidation of In(tfpp)$ClO_4$.

The UV/VIS data for singly reduced In(por)($N_4CR$) are given in Fig. 8 and Table 5 and are similar to the data obtained after reduction of In(por)$ClO_4$ under similar experimental conditions.[20] This may indicate formation of the same singly reduced species for all complexes or could alternatively suggest that UV/VIS spectra of the electroreduced species are independent of the specific axial ligand. Well defined isosbestic points are seen at the beginning of the thin-layer electroreduction for each σ-bonded complex and this indicates the presence of only two spectroscopically detectable species in solution. However, a deviation from isosbestic behaviour gradually appears with time and this is consistent with the occurrence of a slower chemical reaction. Based upon this experimental evidence, it is suggested that a cleavage of the indium–tetrazolato axial ligand bond occurs following the first reduction. The rate of this metal–axial ligand bond cleavage depends upon the nature of the porphyrin ring and is more rapid for the tpp or tfpp species than for those with an oep macrocyclic ring.

The reduction of In(tpp)Cl in $CH_2Cl_2$ gives an ESR spectrum centred at $g = 2.003$.[20] The total width of the signal is equal to 160 G and a splitting of the signal is observed (the width between points of maximum slope is 70 G). This ESR spectrum is very similar to the one obtained after reduction of In(tpp)[$N_4C(CH{=}CHCN)$] (Fig. 9) and, in both cases, suggests formation of a π-anion radical. A splitting of the signal might also be consistent with electron addition at the metal centre but, if this occurred, the hyperfine coupling of the unpaired electron with the nuclear spin of $^{115}In$ ($I = \frac{9}{2}$) should lead to better resolved lines.[20]

The UV/VIS, ESR and electrochemical data are all self-consistent and suggest that tetrazolatoindium(III) complexes are reduced in $CH_2Cl_2$ according to the mechanism shown in Scheme 4.

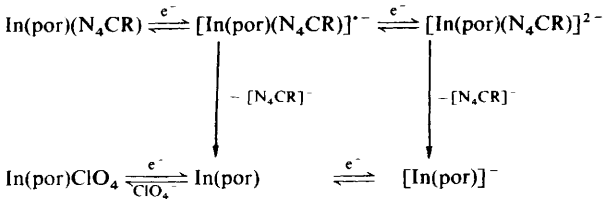


**Scheme 4**

*Oxidation of* In(oep)($N_4CR$) *and* In(tfpp)($N_4CR$).—The spectral evolution which occurs during the first oxidation of In(oep)($N_4CR$) or In(tfpp)($N_4CR$) differs from that of the tpp derivatives (see Fig. 5 and Table 5). The initially intense Soret bands of In(oep)($N_4CR$) and In(tfpp)($N_4CR$) both diminish in intensity and are shifted from 406 to 392 nm for por = oep and from 423 to 412 nm for por = tfpp. The initially sharp Q bands also diminish in intensity and are broadened upon oxidation. The final spectra closely resemble those obtained during electrooxidation of In(oep)$ClO_4$[20] or In(oep)($C_6F_4H$)[32] in PhCN and all three are characteristic of porphyrin π-cation radicals.[33] The UV/VIS spectra of singly oxidized In(oep)[$N_4C(CMe_3)$] and In(oep)[$N_4C(CH{=}CH_2)$] are similar to each other. This could indicate that the oxidation product is the same for both complexes or alternatively that the UV/VIS spectrum of [In(oep)($N_4CR$)]$^+$ is independent of the bound axial ligand.

The first oxidation of In(oep)[$N_4C(CMe_3)$] involves the reproducible abstraction of two electrons on the bulk-electrolysis time-scale, but the ESR spectrum of the resulting solution is consistent with a paramagnetic species. The signal at $g = 2.005$ appears as a singlet and is characteristic of a π-cation radical which does not couple with the metal.[34]

The room-temperature ESR spectrum after oxidation of In(tpp)[$N_4C(CH{=}CHCN)$] has ten well resolved lines (see Fig. 6) which result from a coupling of the unpaired electron with the nuclear spin of $^{115}In$ ($I = \frac{9}{2}$). The signal is centred at $g = 2.002$ and the isotropic coupling constant is 14 G. A hyperfine coupling constant of 3400 G has been reported to result when the electron is added at the indium nucleus.[20] Singly oxidized In(tpp)Cl has a coupling constant of 14 G and this value was suggested to account for a spin density of 0.41% at the metal centre.[20] The unpaired electron in In(tpp)[$N_4C(CH{=}CHCN)$]$^{\bullet+}$ is assumed to be essentially localized at the porphyrin ring π system and the splitting in Fig. 6 can be considered as a superhyperfine coupling between the ring and the metal. A similar spectrum is not observed for the oep derivative because the optical spectrum is typical of an $A_{1u}$ state.[20]

The product formed after bulk electrolysis of In(oep)[$N_4C(CMe_3)$] at +1.7 V is ESR inactive at 120 K, consistent with the presence of a diamagnetic species. A total of 2.8 ± 0.1 electrons are transferred during this oxidation.

Based on the above data, the overall oxidation mechanism shown in Scheme 5 is proposed to occur for the oep and tfpp complexes but not for the tpp species which are more complex and involve isoporphyrin formation as discussed in a following section.

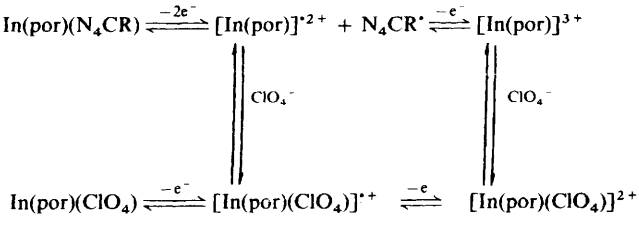


**Scheme 5**

*Isoporphyrin Formation.*—The time-resolved UV/VIS spectra obtained during the first oxidation of In(tpp)[$N_4C(CMe_3)$] differ from those of complexes having an oep or a tfpp ring (see Fig. 5). The intense Soret band of In(tpp)[$N_4C(CMe_3)$] decreases in intensity as the reaction proceeds and progressively shifts from 424 to 413 nm. The Q band at 558 nm becomes less intense and a new band simultaneously appears at 860 nm. A similar long-wavelength band has been reported for doubly oxidized zinc[35–38] and manganese[39] tetraphenylporphyrins and was attributed to the presence of an isoporphyrin.

The data for In(tpp)[$N_4C(CMe_3)$] in Fig. 5 are similar to spectral data obtained after the second oxidation of Zn(tpp) or Mn(tpp)Cl in the presence of a nucleophile[36–39] and suggest that an isoporphyrin is also formed upon oxidation of the indium derivative in $CH_2Cl_2$. The occurrence of a third redox process for each In(tpp)($N_4CR$) complex (Table 4 and Fig. 4) is also in agreement with the three observed oxidations after an isoporphyrin is generated from Zn(tpp) or Mn(tpp)Cl. In these latter two cases, an irreversible reduction may also be seen at a peak potential which is located about 600 mV more negative than $E_p$ for the first oxidation of the complex. This reduction, which is not observed in all cases, is clearly evident in Fig. 11.

The voltammogram in Fig. 11(*a*) was taken after complete

bulk electrolysis of In(tpp)[$N_4C(CMe_3)$] at +1.3 V, after which the potential was scanned to 0.0 V before being reversed. Under these conditions, there is a new reduction at $E_{pc} \approx +0.4$ V. This peak corresponds to the potential expected for reduction of an isoporphyrin.[39] A similar reduction peak is seen in the thin-layer voltammogram of In(tpp)[$N_4C(CMe_3)$] [Fig. 11(*b*)] and this gives further evidence for formation of an isoporphyrin after the first oxidation.

A cleavage of the indium–axial ligand bond has been shown to occur after electrooxidation of In(oep)($N_4CR$) and In(tfpp)($N_4CR$) in $CH_2Cl_2$. A similar behaviour is expected to occur for the tpp analogues and this reaction would be in competition with isoporphyrin formation. The rates of both chemical reactions would be diminished at lower temperatures and this could result in a large shift of the $E_{\frac{1}{4}}$ values as a function of temperature. This shift in $E_{\frac{1}{4}}$ is observed for the second oxidation (see Table 6) and is smaller for the oep and tfpp derivatives, both of which undergo cleavage of the indium–axial ligand bond. However, no isoporphyrin formation is observed under the same experimental conditions.

In summary, the data for oxidation of In(tpp)($N_4CR$) are consistent with isoporphyrin formation and the overall mechanism appears to occur as shown in Scheme 6 where X is a nucleophile.

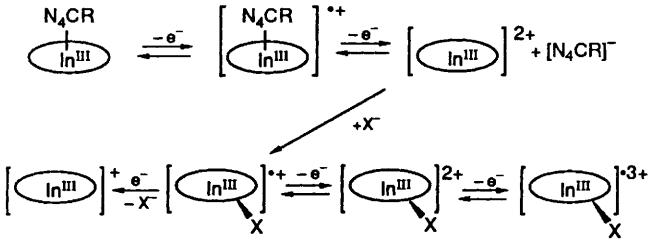


**Scheme 6**

The nature of the nucleophile has not been determined but current studies are now in progress which should help to clarify this point.

## Acknowledgements

The support of the Centre National de la Recherche Scientifique, the National Science Foundation (Grants CHE-8515411 and INT-8412696) and NATO (Grant 0168/87) is gratefully acknowledged.

## References

1 R. Guilard, I. Perrot, A. Tabard, P. Richard, C. Lecomte, Y. H. Liu and K. M. Kadish, *Inorg. Chem.*, 1991, **30**, 27.
2 R. Guilard, N. Jagerovic, A. Tabard, P. Richard, L. Courthaudon, A. Louati, C. Lecomte and K. M. Kadish, *Inorg. Chem.*, 1991, **30**, 16.
3 R. Guilard, S. S. Gerges, A. Tabard, P. Richard, M. A. El Borai and C. Lecomte, *J. Am. Chem. Soc.*, 1987, **109**, 7228.
4 N. Jagerovic, J.-M. Barbe, M. Farnier and R. Guilard, *J. Chem. Soc., Dalton Trans.*, 1988, 2569.
5 J. Geisenberger, J. Erbe, J. Heidrich, U. Nagel and W. Beck, *Z. Naturforsch., Teil B*, 1987, **42**, 55.
6 S. S. Eaton and G. R. Eaton, *J. Am. Chem. Soc.*, 1975, **97**, 3660.
7 M. Bhati, W. Bhatti and E. Mast, *Inorg. Nucl. Chem. Lett.*, 1972, **8**, 133.
8 X. Q. Lin and K. M. Kadish, *Anal. Chem.*, 1985, **57**, 1498.
9 R. Guilard and K. M. Kadish, *Chem. Rev.*, 1988, **88**, 1121.
10 L. J. Bellamy, *The Infrared Spectra of Complex Molecules*, Chapman and Hall, London, 2nd edn., 1980, vol. 2.
11 W. Beck, W. P. Fehlhammer, H. Bock and M. Bauder, *Chem. Ber.*, 1969, **102**, 3637.
12 W. Beck, K. Burger and W. P. Fehlhammer, *Chem. Ber.*, 1971, **104**, 1816.
13 J. C. Weis and W. Beck, *Chem. Ber.*, 1972, **105**, 3202.
14 W. P. Fehlhammer, T. Kemmerich and W. Beck, *Chem. Ber.*, 1979, **112**, 468.
15 P. H. Kreutzer, J. C. Weis, H. Bock, J. Erbe and W. Beck, *Chem. Ber.*, 1983, **116**, 2691.
16 L. L. Garber, L. B. Sims and C. H. Brubaker, Jun., *J. Am. Chem. Soc.*, 1968, **90**, 2518.
17 R. D. Holm and P. L. Donnely, *J. Inorg. Nucl. Chem.*, 1966, **28**, 1887.
18 H. B. Jonassen, J. O. Terry and A. D. Harris, *J. Inorg. Nucl. Chem.*, 1963, **25**, 1239.
19 M. Gouterman, in *The Porphyrins*, ed. D. Dolphin, Academic Press, New York, 1st edn., 1978, vol. 3, p. 1.
20 K. M. Kadish, J.-L. Cornillon, P. Cocolios, A. Tabard and R. Guilard, *Inorg. Chem.*, 1985, **24**, 3645.
21 C. A. Busby and D. Dolphin, *J. Magn. Reson.*, 1976, **23**, 211.
22 R. H. Felton and H. Linschitz, *J. Am. Chem. Soc.*, 1966, **88**, 1113.
23 Z. Dori and R. F. Ziolo, *Chem. Rev.*, 1973, **73**, 247.
24 W. Rigby, P. M. Bailey, J. A. McCleverty and P. M. Maitlis, *J. Chem. Soc., Dalton Trans.*, 1979, 371.
25 T. Kemmerich, J. H. Nelson, N. E. Takach, H. Boehme, B. Jablonski and W. Beck, *Inorg. Chem.*, 1982, **21**, 1226.
26 G. La Monica, G. Ardizzoia, S. Cenini and F. Porta, *J. Organomet. Chem.*, 1984, **273**, 263.
27 P. Paul and K. Nag, *Inorg. Chem.*, 1987, **26**, 2969.
28 W. R. Scheidt, D. A. Summerville and I. A. Cohen, *J. Am. Chem. Soc.*, 1976, **98**, 6623.
29 D. A. Summerville and I. A. Cohen, *J. Am. Chem. Soc.*, 1976, **98**, 1747.
30 N. E. Takach, E. M. Holt, N. W. Alcock, R. A. Henry and J. H. Nelson, *J. Am. Chem. Soc.*, 1980, **102**, 2968.
31 K. M. Kadish, *Prog. Inorg. Chem.*, 1986, **34**, 435.
32 A. Tabard, R. Guilard and K. M. Kadish, *Inorg. Chem.*, 1986, **25**, 4277.
33 R. H. Felton, in *The Porphyrins*, ed. D. Dolphin, Academic Press, New York, 1st edn., 1978, vol. 5, p. 53.
34 J. Fajer and M. S. Davis, in *The Porphyrins*, ed. D. Dolphin, Academic Press, New York, 1st edn., 1978, vol. 4, p. 197.
35 D. Dolphin, R. H. Felton, D. C. Borg and J. Fajer, *J. Am. Chem. Soc.*, 1970, **92**, 743.
36 J. A. S. Cavaleiro, B. Evans and K. M. Smith, in *Porphyrin Chemistry Advances*, ed. F. R. Longo, Ann Arbor Science Publishers, Ann Arbor, MI, 1979, p. 335.
37 J. A. Guzinski and R. H. Felton, *J. Chem. Soc., Chem. Commun.*, 1973, 715.
38 K. M. Kadish and R. K. Rhodes, *Inorg. Chem.*, 1981, **20**, 2961.
39 A. S. Hinman, B. J. Pavelich and A. E. Kondo, *J. Electroanal. Chem., Interfacial Electrochem.*, 1987, **234**, 145.

*Received* 27*th November* 1991; *Paper* 1/06016C